A Comparison of Controllers for the Quadruple Tank System

Grebeck, Michael

1998

Document Version:
Publisher's PDF, also known as Version of record

ISSN 0280–5316
ISRN LUTFD2/TFRT--7576--SE

A Comparison of Controllers for the Quadruple Tank System

Michael Grebeck
California Institute of Technology

Department of Automatic Control
Lund Institute of Technology
August 1998

Department of Automatic Control
Lund Institute of Technology
Box 118
S-221 00 Lund Sweden

Document name
INTERNAL REPORT

Date of issue
August 1998

Document Number
ISRN LUTFD2/TFRT--7576--SE

Author(s)
Michael Grebeck

Supervisor
Karl Henrik Johansson and Anders Rantzer

Sponsoring organisation

Title and subtitle
A Comparison of Controllers for the Quadruple Tank System.

Abstract

This paper makes an experimental comparison of several different control methods evaluated on the quadruple tank process. The quadruple tank process is a multivariable process designed such that a zero can be moved between the left and right half planes allowing performance limitations to be examined. The five different control methods studied in this paper include Linear Quadratic Gaussian (LQG), H-Infinity, loop-shaping, feedback linearization, and model predictive control (MPC). The experimental comparisons were made with respect to step responses and disturbance rejections for both the minimum and nonminimum phase plants.

Key words
Multivariable process; Multivariable zero; Right half plane zero; Performance limitations

Classification system and/or index terms (if any)

Supplementary bibliographical information

ISSN and key title
0280–5316

ISBN

Language
English

Number of pages
30

Recipient's notes

Security classification

1. Introduction

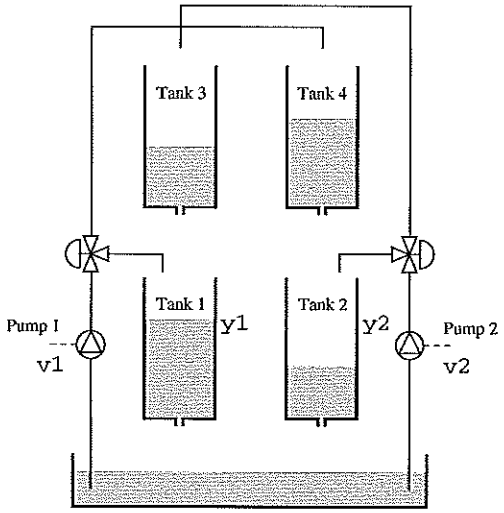

The quadruple tank process is a two-input, two-output system with a movable zero composed of an interconnection of two double tank processes. For a full description of this process and the work already completed on it, see Karl Henrik Johansson's paper "A Multivariable Process with an Adjustable Zero" (1997). The two inputs are the voltages to the two water pumps, and the two outputs are the water levels of the two lower tanks. In addition, there are valves between the pumps and the tanks. By adjusting these valves, the proportions of flow going to the upper and lower tanks is changed, thereby moving the zero. This movable zero is located on the real axis and can be moved between the left and right half planes.

The main purpose of this paper is to illustrate how right half plane (RHP) zeros limit performance for a multivariable process. The reader should see *Fundamental Limitations in Filtering and Control* (1997) by Seron, Braslavsky, and Goodwin for a full treatment of RHP zero performance limitations. As is well known for single-input-single-output (SISO) systems, if any RHP zero lies within the closed loop bandwidth, problems will occur with any control law. In other words,

$$\text{a zero at } z = \alpha \quad \Rightarrow \quad \omega_b \lesssim \alpha$$

Therefore, the only option is to reduce the bandwidth and hope that the responses obtained at lower frequencies are adequate. As the experimental data will show, nonminimum phase controllers which do produce stable responses have small bandwidths compared to that of the minimum phase controllers. Control laws which attempt arbitrarily good tracking for the nonminimum phase plant will be unstable. From the view of the linearized dynamics, the only way perfect tracking can be obtained when a right half plane zero exists is if there is an unstable pole-zero cancellation. Another way the theoretical effects of RHP zeros are illustrated is with the *water-bed effect*:

$$\sup_{\omega \in [\omega_1, \omega_2]} |S(j\omega)| \geq \frac{1}{\|S\|_\infty^m}$$

where m is a positive constant and the system contains a zero in the open RHP. This theorem states that if the magnitude of the sensitivity function is made small in one frequency range, it must necessarily be large in another range.

In the multivariable case, zeros also have a direction associated with a location. If there exists a multivariable zero at $z = \alpha$, then the transfer matrix $G(s)$ loses rank at $z = \alpha$. In addition, there is a direction vector ψ such that

$$\begin{bmatrix} G_{11}(\alpha) & G_{12}(\alpha) \\ G_{21}(\alpha) & G_{22}(\alpha) \end{bmatrix} \begin{bmatrix} \psi_1 \\ \psi_2 \end{bmatrix} = 0.$$

Provided that ψ is not in the direction of a unit vector, the effects of a RHP zero can be distributed among more than one output. As a consequence, the performance limitations of a RHP zero for a MIMO system are not as great as in a SISO system.

In addition, the dynamics for the process are nonlinear which provides for different control methods to be studied: equilibrium point linearization, feedback linearization, and model predicted control. Therefore, comparisons can be made between controllers based on linearized and non-linearized dynamics.

The remainder of this paper is divided as follows: Section 2 contains the system dynamics about which the controllers are designed, Section 3 makes some technical comments about the process, Section 4 contains the description of the design techniques for each of the controllers, Section 5 makes comparisons of the experimental data, and then Section 6 makes the concluding remarks.

2. Dynamics

The following are the system dynamics for the quadruple tank system.

$$\dot{h_1} = -\frac{a_1}{A_1}\sqrt{2gh_1} + \frac{a_3}{A_1}\sqrt{2gh_3} + \frac{\gamma_1 k_1}{A_1}u_1, \tag{1}$$

$$\dot{h_2} = -\frac{a_2}{A_2}\sqrt{2gh_2} + \frac{a_4}{A_2}\sqrt{2gh_4} + \frac{\gamma_2 k_2}{A_2}u_2, \tag{2}$$

$$\dot{h_3} = -\frac{a_3}{A_3}\sqrt{2gh_3} + \frac{(1-\gamma_2)k_2}{A_3}u_2, \tag{3}$$

$$\dot{h_4} = -\frac{a_4}{A_4}\sqrt{2gh_4} + \frac{(1-\gamma_1)k_1}{A_4}u_2, \tag{4}$$

where each $\gamma_i \in [0, 1]$ is set by the valves and determines the plant phase, and k_i are the pump gains.

After solving for the equilibrium points u_i^o and h_i^o, make the change of variables $x_i = h_i - h_i^o$ and $w_i = u_i - u_i^o$ and the linearization becomes

$$\dot{x} = \begin{pmatrix} \frac{-1}{T_1} & 0 & \frac{A_3}{A_1 T_3} & 0 \\ 0 & \frac{-1}{T_2} & 0 & \frac{A_4}{A_2 T_4} \\ 0 & 0 & \frac{-1}{T_3} & 0 \\ 0 & 0 & 0 & \frac{-1}{T_4} \end{pmatrix} x + \begin{pmatrix} \frac{\gamma_1 k_1}{A_1} & 0 \\ 0 & \frac{\gamma_2 k_2}{A_2} \\ 0 & \frac{(1-\gamma_2)k_2}{A_3} \\ \frac{(1-\gamma_1)k_1}{A_4} & 0 \end{pmatrix} w,$$

$$y = \begin{pmatrix} 1 & 0 & 0 & 0 \\ 0 & 1 & 0 & 0 \end{pmatrix} x,$$

A_1,A_3	[cm^2]	28
A_2,A_4	[cm^2]	32
a_1,a_3	[cm^2]	0.071
a_2,a_4	[cm^2]	0.057
g	[cm/s^2]	981

Table 1 Parameter values for the physical experiment.

where

$$T_i = \frac{A_i}{ai}\sqrt{\frac{2h_i^o}{g}}.$$

Notice there is no longer the k_c term in the linearized C matrix. The conversion from volts to the tank heights is dealt with in the software, so k_c is no longer necessary.

The phase of the plant is determined by γ_i. If $1 < \gamma_1 + \gamma_2 < 2$, the phase is minimum. If $1 < \gamma_1 + \gamma_2 < 2$, one of the plant zeros moves along the real axis into the right half plant, so the phase is nonminimum. If $\gamma_1 + \gamma_2 = 0$, the zero is located at the origin, and the equilibrium tank flows through Tank 1 and Tank 2 are dependent.

3. Notes on Hardware,Software,and the Physical Process

The newly rebuilt quadruple tank process has the added benefit that the phase of the controller can be changed by the flip of a couple switches. When valves one and three are on, the phase is minimum. When valves two and four are on, the phase is nonminimum. And when all four valves are on, the movable zero is usually located very near the imaginary axis.

The equilibrium points for a given phase are often not very consistent from day to day. Table 1 shows the range of values for each γ_i and each pump gain k_i. Due to these large variations in the physical process, it becomes necessary to measure γ_i and k_i each day, and then design a controller around the measured parameters for that day. The parameters do not vary too much within a given day. Because of this fact, the different controllers in this paper are designed around the equilibrium point the day the data was taken. Therefore, step response were done at slightly different heights.

A second problem with the physical process occurs during the start-up. Occasionally, there is a back-flow problem with the valves after the pumps have been off. The result is that all the water flows into only one of the tanks. In this case, it is recommended that the pump voltage is turned on high for a couple of seconds and then turned back down to the equilibrium level. Therefore, it is necessary to watch the more aggressive controllers which reduce the input voltage(s) to zero. If the input voltage is at zero for a long enough period, this back-flow problem could occur during a control action.

All controllers in this paper were implemented in dSPACE, not the In-Touch interface used for the already documented decentralized PI controllers.

	Valves 1,3 (minimum)	Valves 2,4 (non-minimum)	Valves 1,2,3,4 (imag axis pole)
γ_1	0.60 - 0.70	0.30 - 0.40	0.44-0.50
γ_2	0.60 - 0.70	0.30 - 0.40	0.50-0.56
k_1	2.7 - 3.4	2.7 - 3.4	3.0 - 3.5
k_2	2.7 - 3.4	2.7 - 3.4	3.0 - 3.5

Table 2 Measured tank parameters on the physical process.

The benefit of dSPACE is that nonlinear control can be implemented through S-Functions in the simulink diagrams. S-Functions were used in the case of feedback linearization and model predictive control. Another benefit is that linear controllers can be loaded in as .mat files. This is extremely useful when controllers have more than a few states. One drawback with dSPACE is that no easy way to reset the linear controller states was found. This can cause problems if you restart a controller with integrators which previously had large errors. If this is the case, it is necessary to down-load the dsp again.

The data for most controllers includes the experimental responses and the nonlinear simulation responses. The nonlinear simulation were done directly in Simulink with S-Functions, not in the InTouch interface previously used with the decentralized PI controllers.

Excluding model predictive control, all controllers in this paper were ran at a sampling period of .2 seconds. This is faster than the sampling period of 1 second previously used. In the case of model predictive control, a sampling period of 1 second was necessary for the additional computation time.

The output measurement for the water level of each tank (v_i) is given in volts. There is an approximate factor of 20 between this measurement and the water height. In addition, a small offset is added in. Both of these values vary from day to day. The variance in the factor of 20 is relatively small, and therefore it can be assumed to remain unchanged. The offset not only varies from day to day but from experiment to experiment. This offset ranges in value from -.6 cm to 2 cm. Setting this value is necessary every time the experiment is ran.

$$h_i = a_i v_i + b_i \qquad \text{where } a_i \approx 20 \text{ cm/V and } -0.6 \text{ cm} < b_i < 2 \text{ cm}$$

Finally, the tank labels on the physical system were changed. Tank 1 corresponds to Tank 1b, Tank 2 to Tank 2b, Tank 3 to Tank 1a, and Tank 4 to Tank 2a.

4. Control methods

There are five different control schemes studied, and each was examined on the minimum and nonminimum phase plant. Most design techniques used the linearized model given in section 2, or an augmented version of this model. Feedback linearization was the only method based on the full nonlinear dynamics.

All linear designs use a controller of the form:

$$K(s) = \begin{bmatrix} K_{11}(s) & K_{12}(s) \\ K_{21}(s) & K_{22}(s) \end{bmatrix}.$$

No other limitations were placed on the structure or the order of the controllers.

4.1 Linear Quadratic Gaussian Control

The first Linear Quadratic Gaussian (LQG) controllers were designed using the separation principle with Matlab's LQE and LQR commands which allows the principal gains to be shaped. Controllers were also designed directly using the LQG Matlab command on the plant and also on a plant augmented with integrators.

LQG Design Method 1 Design by the separation principle contains two steps:

- Construct a Kalman filter to obtain the optimal state estimate.
- Solve the deterministic linear quadratic problem.

The performance specifications are considered by the design in the first step: The open loop principal gains of the Kalman filter are shaped to produced a satisfactory return ratio. The second step involves recovery of the return ratio of the Kalman filter at the output and has an effect of a tuning knob: As the knob is turned, the principal gains of $G(s)K(s)$ will approach the open loop principal gains of the Kalman filter.

A Kalman filter produces the optimal states estimate for the plant:

$$\begin{aligned} \dot{x} &= Ax + Bu + Gw \\ y &= Cx + Du + v \end{aligned}$$

where the process noise w has covariance Q_1 and the measurement noise v has covariance R_1. As the first design step for the minimum phase case, a Kalman filter was constructed where disturbances on the plant were assumed to act through the input, and Q_1 and R_1 were chosen to be identity matrixes. Figure 1 shows the principal gains of the return ratio for this filter. Both have a small constant gain at low frequency which will result in steady-state error. To solve this problem, two poles placed at $s = -.0001$ were augmented into the plant. A Kalman filter was then designed about the augmented plant. Figure 2 shows the new singular values for the return ratio. The integral action worked in raising the gain at $\omega = 0$. Using singular value decomposition, the process noise covariance Q_1 was modified to raise the lower principal gain up to the higher principal gain to improve more on the steady-state error. Figure 3 shows the new principal gains.

The second step of solving the deterministic linear quadratic control problem involves finding the gain matrix such that the state-feedback minimizes the cost function:

$$\lim_{T\to\infty} E\left\{ \int_0^T \left(x^T Q_2 x + u^T R_2 u\right) dt \right\}.$$

The Q_2 matrix was chosen such that weight was placed on h_1 and h_2, and R_2 was chosen such that $R_2 = \rho I$. As ρ is decreased, the principal gains of

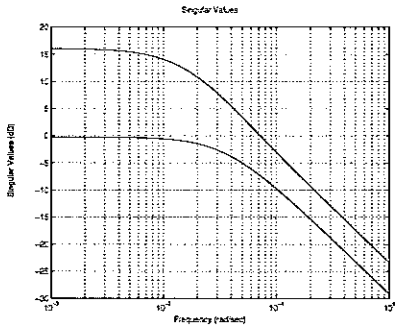

Figure 1 Minimum Phase LQG 1: Principal gains of return ratio using the non-augmented plant.

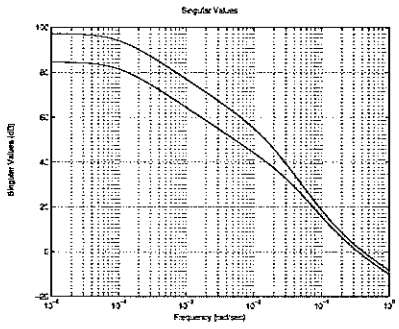

Figure 2 Minimum Phase LQG 1: Principal gains of return ratio using the augmented plant.

$G(s)K(s)$ will approach the open loop principal gains of the Kalman filter, and the return ratio of the Kalman filter will be recovered at the output. Figure 4 shows the principal gains of the sensitivity function $S(s)$ and the closed loop transfer function $T(s)$ for the final control design.

The same method was used to design a controller for the nonminimum phase plant. LQG compensators are known to have problems with right half plane zeros, and the only hope is that the RHP zero does not lie too far within the bandwidth. Therefore, weights on the covariance matrixes were adjusted, reducing the bandwidth, such that stable responses were obtained.

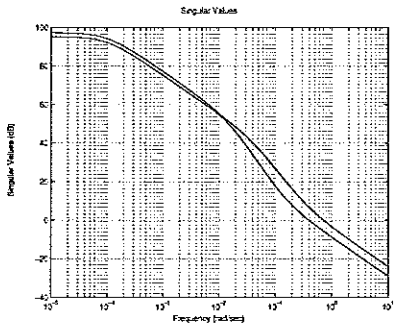

Figure 3 Minimum Phase LQG 1: Principal gains of return ratio with modified Q_1.

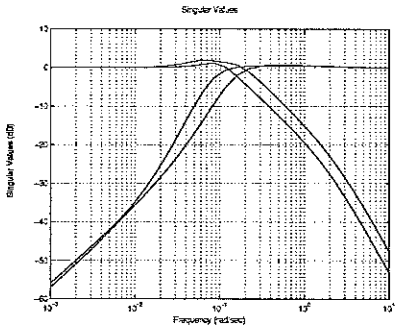

Figure 4 Minimum Phase LQG 1: Principal gains of S(s) and T(s).

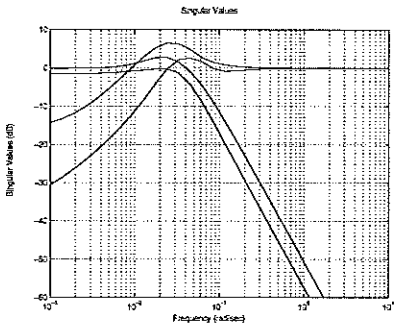

Figure 5 Non-Minimum Phase LQG 1: Principal gains of S(s) and T(s).

More specifically, unstable responses were obtained when ρ was reduced beyond a certain value. Figure 5 shows the principal gains of the sensitivity and closed loop transfer functions.

Two points should be made about the plots of $S(s)$ and $T(s)$:

- The reduction in bandwidth due to the RHP zero is very clear.
- For the nonminimum phase system, the movable zero is located at $z = .017$, which is slightly within the bandwidth. As a result, a hump in the sensitivity function near the zero is evident. If the bandwidth is pushed out farther, this hump will increase and eventually result in an unstable system.

LQG Design Method 2 LQG controllers were then designed for the minimum phase plant directly with Matlab's LQG command. As Figure 1 illustrated, a DC offset should be expected for the non-augmented minimum phase plant. The weighting matrix W was chosen such that the cost function place a heavy weight on the error of h_1 and h_2, and very little weight on the error of h_3 and h_4. Figure 6, which shows the sensitivity and closed loop transfer function of the resulting controller, also verifies the DC offset.

An LQG controller was also constructed with the non-augmented, nonminimum phase plant. Although stable, this LQG design method was not very successful as Figure 7 illustrates. At low frequency, the smallest principal gain of $T(s)$ is far less than one. Therefore, DC offsets will be extremely bad. Also, the principal gains of the sensitivity are large at low frequency, which will result in very poor disturbance rejection. This controller was not tested on the physical experiment because of its poor characteristics.

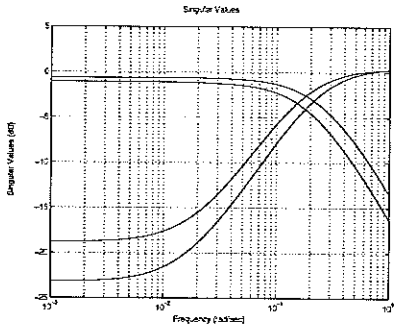

Figure 6 Minimum Phase LQG 2: Principal gains of S(s) and T(s).

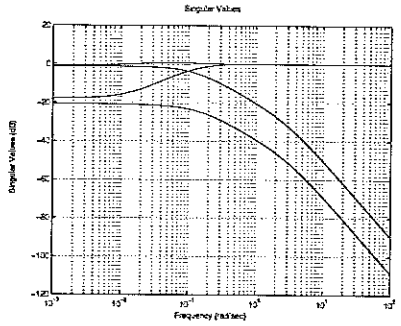

Figure 7 Non-Minimum Phase LQG 2: Principal gains of S(s) and T(s).

LQG Design Method 3 As can be seen from the singular value plots, using Matlab's LQG command on the plant augmented with integrators makes significant improvements to both the minimum and nonminimum phase plant. The weighting matrix W for the cost function placed small weight on the errors of h_3 and h_4, large weight on the errors of h_1 and h_2, and very large weight on the integral of the errors of h_1 and h_2.

4.2 H_∞

H_∞ controllers were designed for both the minimum and nonminimum phase plants using Matlab's μ-Analysis and Synthesis Toolbox.

The uncertainty in the plant comes from three main areas:

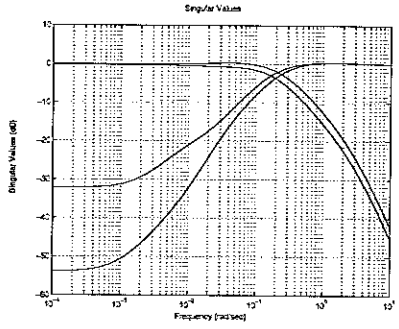

Figure 8 Minimum Phase LQG 3: Principal gains of S(s) and T(s).

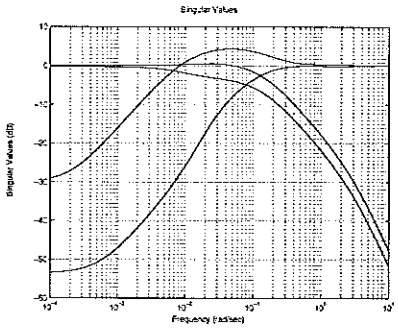

Figure 9 Non-Minimum Phase LQG 3: Principal gains of S(s) and T(s).

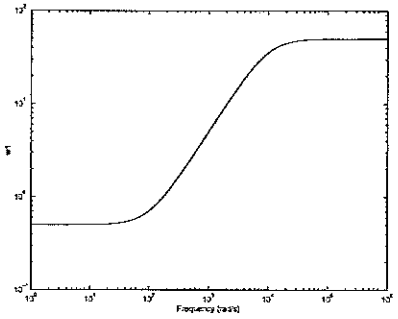

Figure 10 Uncertainty Weighting Function W_1 for both minimum and nonminimum phase.

- The inconsistent γ_i and k_i produce significant variations in the equilibrium points. Therefore, the controller will probably be operating at a different equilibrium point than the one it was designed about.
- Besides normal sensor noise, the measurement of the tank heights are fairly inaccurate in other ways. As already mentioned, it is necessary to set a bias value every time the experiment is tested, but this value can also change noticeable during the experiment. For example, the capacitor above the water level could initial be dry, but as the water level raises and lowers, some moisture is left on the capacitor above the water level. This has been seen to change the bias value.
- The nonlinear terms in the dynamics besides other common nonlinearities such as input saturations and time delay.

This overall plant uncertainty is lumped together and modeled as multiplicative uncertainty. For both the minimum and nonminimum phase plants, the uncertainty weight, W_1, allowed for up to a 50% modeling error at DC and increases with frequency.

In Matlab, the nominal performance requirements are specified by a transfer function W_2. The inverse of this transfer function gives the desired upper bound on $S(s)$. The weighting function for this design desires no more than a 3.3% error at steady-state, and this performance requirement decreases at higher and higher frequencies. The weighting function for the nonminimum case was chosen such that the performance requirements become less stringent at lower frequencies than the weighting function for the minimum phase

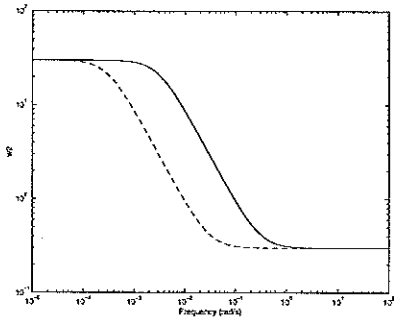

Figure 11 Performance Weighting Function W_2 for both minimum (solid) and non-minimum (dashed) phase.

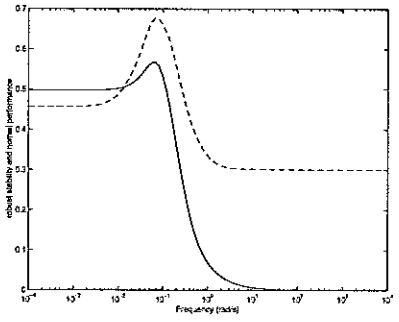

Figure 12 Minimum Phase H_∞: Robust Stability (solid) and Nominal performance (dashed).

case. More specifically, the nonminimum phase sensitivity specifications becomes less stringent faster by a factor of ten. As a result, the bandwidths of the two different controllers differ by an approximate factor of ten. See figure 11 for the the weighting functions, W_2, of both phases.

Two disturbances were modeled on the outputs to the plant, h_1 and h_2. The suboptimal H_∞ controller for the minimum phase plant was produced in Matlab such that the ∞-norm of the transfer function from the perturbation inputs and disturbances to the perturbation outputs and errors is internally stable and minimized. Figure 12 shows the frequency response of $W_2(I+GK)^{-1}$ and $W_1KG(I+KG)^{-1}$, where K is the controller and G is the plant model. It follows from these plots that the controller meets the robust stability requirements since $\|W_2(I+GK)^{-1}\|_\infty < 1$ and nominal performance requirements since $\|W_1KG(I+KG)^{-1}\|_\infty < 1$.

Using μ-Synthesis, robust performance is checked. Figure 13 shows that $\|W_2(I+GK)^{-1}\|_\infty > 1$. Therefore, it follows that this controller does not achieve robust performance. D-K iteration was completed in Matlab and a new controller was designed. D-K iteration works by concentrating the H_∞ minimization across certain frequencies, and as a result, the order of the controller is greatly increased. The H_∞ controllers used in this paper contain up to 28 states. Figure 13 shows that this controller does achieve robust performance.

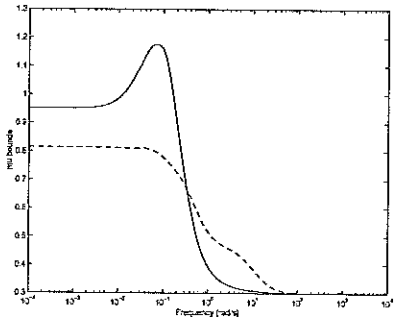

Figure 13 Minimum Phase H_∞: Robust Performance before D-K iteration (solid) and after (dashed).

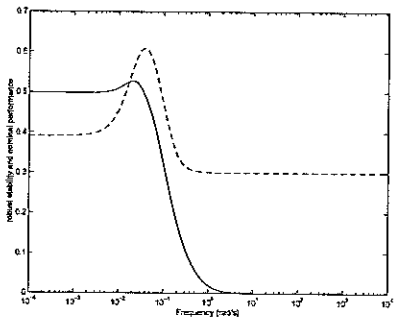

Figure 14 Nonminimum Phase H_∞: Robust Stability (solid) and Nominal performance (dashed).

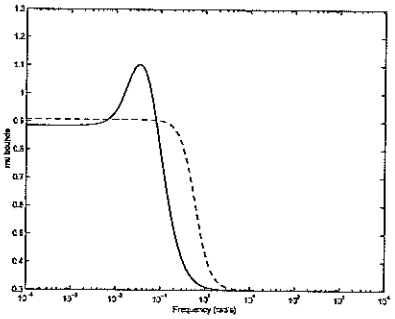

Figure 15 Nonminimum Phase H_∞: Robust Performance before D-K iteration (solid) and after (dashed).

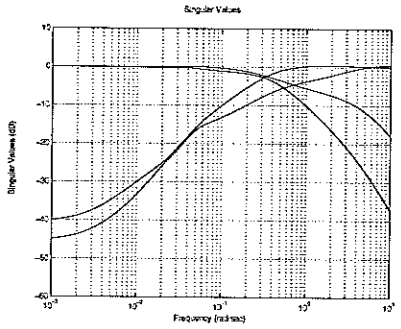

Figure 16 Minimum Phase H_∞: Principal Gains of $S(s)$ and $T(s)$.

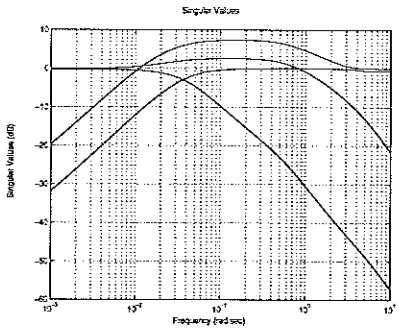

Figure 17 Nonminimum Phase H_∞: Principal Gains of $S(s)$ and $T(s)$.

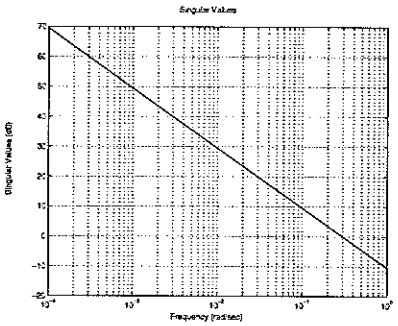

Figure 18 Nonminimum Phase Desired L.

4.3 Loop-Shaping

The general idea behind simple loop-shaping methods is to construct an open loop transfer function L which meets desired performance requirements. The controller is then obtained from the plant by C=L/P. This method should work provided the plant has no RHP zeros. Otherwise, there will be unstable pole-zero cancellations in the system. There are more advanced methods of loop-shaping to deal with RHP zeros, but they were not pursued here. This simple method of loop-shaping illustrates how easy controller design is for minimum phase plant. The response which the minimum phase controller produces is comparable to the other control methods, and this loop-shaping controller is the lowest order (4) of all controllers documented in this paper.

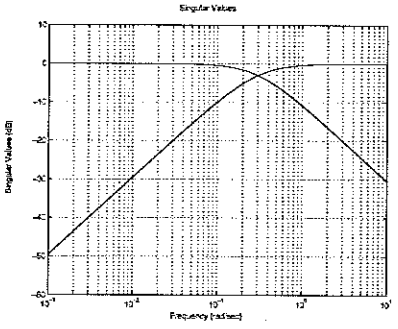

Figure 19 Minimum Phase Loop-Shaping: Principal Gains of $S(s)$ and $T(s)$.

4.4 Feedback Linearization

Feedback linearization was attempted on the quadruple tank system with full state feedback and the control law:

$$u_1 = \frac{A_1}{\gamma_1 k_1}\Big(-\alpha_1\big(h_1 - h_{1,d}\big) - \frac{a_3}{A_1}\sqrt{2gh_3} + \frac{a_1}{A_1}\sqrt{2gh_1}\Big)$$

$$u_2 = \frac{A_2}{\gamma_2 k_2}\Big(-\alpha_2\big(h_2 - h_{2,d}\big) - \frac{a_4}{A_2}\sqrt{2gh_4} + \frac{a_2}{A_2}\sqrt{2gh_2}\Big)$$

where $h_{i,d}$ is the desired height in Tank i and α_i is chosen to be a positive constant. In both simulations and on the experiment, a value of .2 was used for α_1 and α_2. The resulting closed loop dynamics from this control law are

$$\dot{h_i} + \alpha_i\big(h_i - h_{i,d}\big) = 0 \qquad \text{for } i = 1, 2$$

Obviously, h_1 and h_2 are stable, but as the phase of the plant changes from minimum to nonminimum, the internal dynamics on h_3 and h_4 become unstable. The unstable internal dynamics of the nonminimum phase plant can be seen by the nonlinear simulation results in Figure 16. The dynamics of h_1 and h_2 can become arbitrarily good (in simulation) by adjusting α_i, but for nonminimum phase systems, infinite control energy is needed for perfect tracking. The plots show that h_1 and h_2 produce excellent responses, but in order to hold these heights, u_1 must tend towards $-\infty$ and u_2 must tend toward $+\infty$. The result is that the water level in Tank 4 tends towards ∞ and the level in Tank 3 tends towards $-\infty$. On the physical systems, since negative control inputs do not exist and since it is impossible to have negative water heights, Tank 3 will empty and then Tank 1 will eventually begin to overflow. As u_1 is increasing indefinitely (or at least to saturation), Tanks 2 and 4 will also overflow.

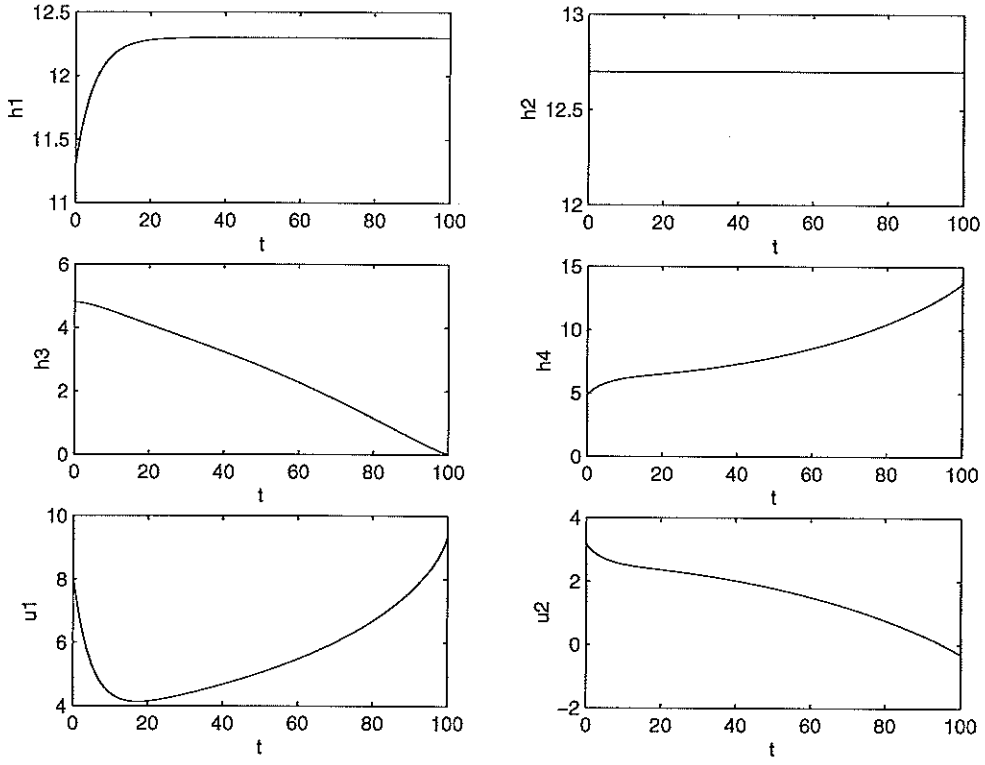

Figure 20 Nonminimum Phase Feedback Linearization: nonlinear simulation results.

4.5 Model Predictive Control

The design of the first MPC controller contains an algorithm which predicts only one step into the future and attempts to minimized $\|e^1_{1,2}\|_2$, where $e^1_{1,2} = (e^1_1, e^1_2)$ and e^i_k is the error in tank k at i steps in the future. The algorithm which computes the minimum of $\|e^1_{1,2}\|_2$ loops through each input value at multiples of .1 volts, and it predicts the output using the linearized model. This algorithm is extremely inefficient and is unable to solve for more than one step into the future without exceeding available computation time. Therefore, this MPC controller produces poor results in even the minimum phase plant. The responses contain very large oscillations which are the likely result from predicting only one step into the future: The controller attempts to reach the desired position in only one step without any consideration of overshoot at the next step. In fact, the oscillations would eventually start to grow, and this controller becomes unstable. This MPC control algorithm tested on the nonminimum phase system not only has the same large oscillations at the output, but it also gives the appearance of unstable internal dynamics. The error function only tries to minimize the errors on h_i and h_2, so h_3 and h_4 are permitted to go unstable. These unstable dynamics are very similar to the unstable internal dynamics found in feedback linearization of the nonminimum system. The MPC controller attempts perfect tracking, but this is impossible for nonminimum systems.

Matlab has many optimization routines which can be used to produce better results in simulations. Unfortunately, these commands are not supported by rtw and dSPACE to run in real-time. A second MPC real-time algorithm was written on the concept of direction of steepest decent. The problem is to solve the equation:

$$\text{minimize } E(u) = \sum_{i=1}^{n} \left(\alpha \left\| e^i_{1,2} \right\|_2 + \beta \left\| u^i \right\|_2 \right)$$

subject to

$$0 < u^i_k < 10$$

where e^i and u^i are the errors and inputs at i steps into the future, n is the total number of steps into the future for which the error function will be evaluated, and α and β are constants which will determine the shape of the response. As stated earlier, the sampling time of this controller is 1 second, so n also corresponds to the number of seconds which are predicted.

Given an initial set of inputs, the gradient of the error function is solved numerically, and a step is taken in the direction of the input with the most negative derivative. If any of the input values, u^i_k, attempted to go outside the allowable bounds, the error function was minimized with that input value set equal to the appropriate saturation value. Since the error function is quadratic in u, there should be no problem with multiple extrema. Predictions were again based on the linearized model.

This algorithm was much more efficient and produced good responses for the minimum phase system. At most, the experiment was tested with $n = 20$, but anything beyond $n = 5$ produced very similar results for given values of α and β. The values of these constants which were tested are $\alpha = 40$ and $\beta = .5, 1, 2, 3$. The choice of these constants determines the shape of

the response. A smaller value of β will result in very fast responses with large overshoot and oscillations. Increasing β will solve the problems with overshoot and oscillations, but at the expense of rise time and DC offset. Since β penalizes any difference in control energy from the equilibrium, this DC offset is to be expected as β is increased relative to α. Therefore, setting β equal to a large value will result in a slow, smooth response with no overshoot and a large DC offset.

This MPC algorithm modified for the nonminimum phase plant was found to be unsuccessful. The same problem arises as in the first MPC algorithm: Since only the errors on Tanks 1 and 2 are minimized, Tanks 3 and 4 are permitted to go unstable while Tanks 1 and 2 have very good tracking (until input saturations were reached). For this MPC nonminimum phase controller, tracking on Tanks 1 and 2 is fast enough that n is not a large factor. Again, any values beyond $n = 5$ produces a similar response. On the physical system u_1 grows toward positive saturation and u_2 grows toward negative saturation. As a result, Tank 3 empties, Tank 4 overflows, and Tanks 1 and 2 have very good tracking until the input saturations were reached.

The nonminimum phase MPC algorithm was then modified to minimize the function

$$E(u) = \sum_{i=1}^{n} \left(\alpha \left\| e_{1,2}^{i} \right\|_2 + \eta \left\| e_{3,4}^{i} \right\|_2 + \beta \left\| u^{i} \right\|_2 \right)$$

where the new parameter η is the weight given to the 2-norm of the errors on Tanks 3 and 4. The values tested for η were in the range from three to ten. This nonminimum phase MPC algorithm was also found to be unsuccessful: Due to limits on computation time, the software crashed at values of n around 25 seconds. This method is expected to work if there exists sufficient computation time and more efficient algorithms. Based on the responses of other controllers for the nonminimum phase plant, software and hardware which can support computations with $n = 200$ (or perhaps more) can be expected to yield reasonable results. Using this MPC algorithm with smaller values of n, for example $n = 15$, produced extremely large steady-state errors in all tanks.

5. Summary of experimental results

The control methods were tested experimentally in two different ways:

- Tracking. The trajectory is a step in h_1 while h_2 is held constant. This is performed after the system reaches equilibrium.
- Disturbance Rejection. A small cup of water is poured into h_2 after the system reaches equilibrium. This corresponds to an approximate five centimeter increase in h_2.

The results of each controller to the above is shown in a figure with four plots. The upper left plot shows h_1 measured in centimeters, the upper right plot shows h_2 measured in centimeters, the lower left plot shows u_1 measured in volts, and the lower right plot shows u_2 measured in volts. The plots of the step responses also include nonlinear simulation results besides the experimental results. The disturbance rejection plots only contain the experimental results since the disturbance is hard to accurately simulate in Simulink. The results

symbol	description	units
t_r	Rise time	sec
M_p	Overshoot	percent
t_s	Settling time	sec
ss e_1	Steady-state error in Tank 1	percent
$\|e_i\|_2$	$\sqrt{\sum_{k=0}^{n}(h_i^k - h_{i,d})^2}$	
$\|e_i\|_\infty$	$\max_{0\le k\le n} \|h_i^k - h_{i,d}\|$	

Table 3 Description and units of parameters used to evaluate the experimental data.

	LQG 1	LQG 2	LQG 3	H_∞	lp-shp	fbk lin	MPC $\beta = .5$	MPC $\beta = 2$
t_r	8	12	10	7	8	12	4	13
M_p	30	5	10	8	10	0	35	5
t_s	120	70	65	50	55	25	35	50
ss e_1	0	5	1	0	0	3	0	3
$\|e_1\|_2$	3.4	2.7	2.5	1.9	2.2	2.6	2.0	2.4
$\|e_1\|_\infty$	1.0	1.0	1.0	1.0	1.0	1.0	1.0	1.0
$\|e_2\|_2$	1.1	1.1	1.1	0.6	0.7	0.9	0.7	1.0
$\|e_2\|_\infty$	0.2	0.2	0.2	0.1	0.1	0.1	0.1	0.2

Table 4 Experimental data for the step response in h_1 for the minimum phase plant.

for all controllers are listed in a table for direct comparison. Because of sensor noise, some of the characteristics, such as settling time, are hard to measure, so approximations were made. Table 3 describes the characteristics measured for each controller.

5.1 Tracking

Minimum Phase Table 4 illustrates the individual characteristics of the minimum phase step responses. Some of the notable items are:

- MPC with $\beta = .5$ produced a very fast response. As a consequence, the overshoot was large.
- The plots of feedback linearization seem to indicate a small DC offset. Increasing α_i should speed up the response and eliminate the offset.
- In terms of minimizing the error norms, H_∞ produced the best response.
- As expected with MPC, increasing β slowed down the response, reduced the oscillations, and created a DC offset.

Nonminimum Phase Below, Table 5 lists the experimental characteristics of the step responses for all the stable, nonminimum phase controllers. The

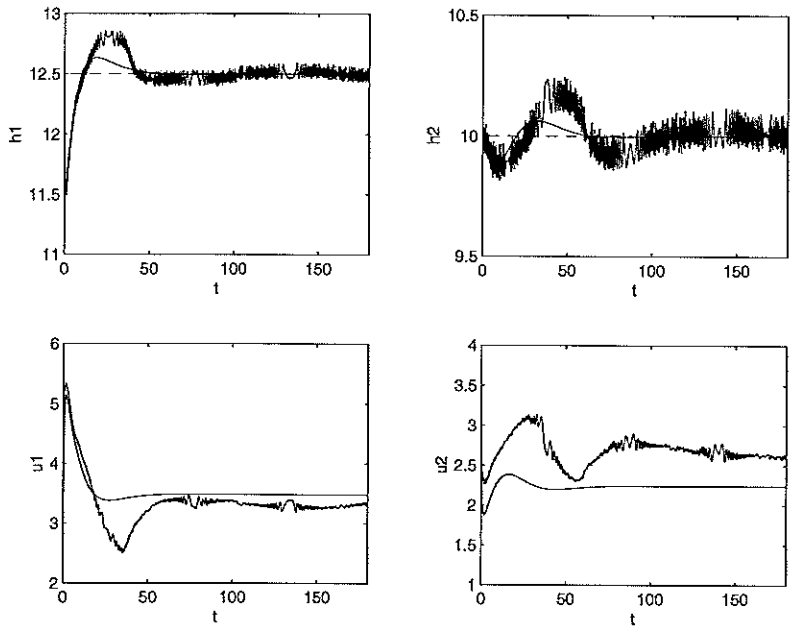

Figure 21 Minimum Phase LQG 1 Step Response: nonlinear model and the experiment.

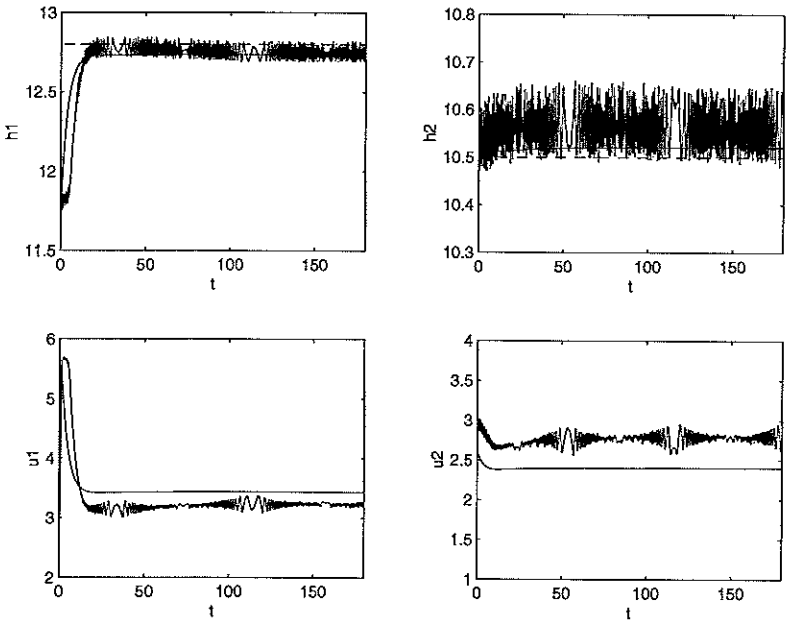

Figure 22 Minimum Phase LQG 2 Step Response: nonlinear model and the experiment.

most unexpected item is that the H_∞ controller produced the worst response in terms of minimizing the error norms. The weighting functions used in the design were then modified in an attempt produce error norms better than that of LQG methods, but to no avail.

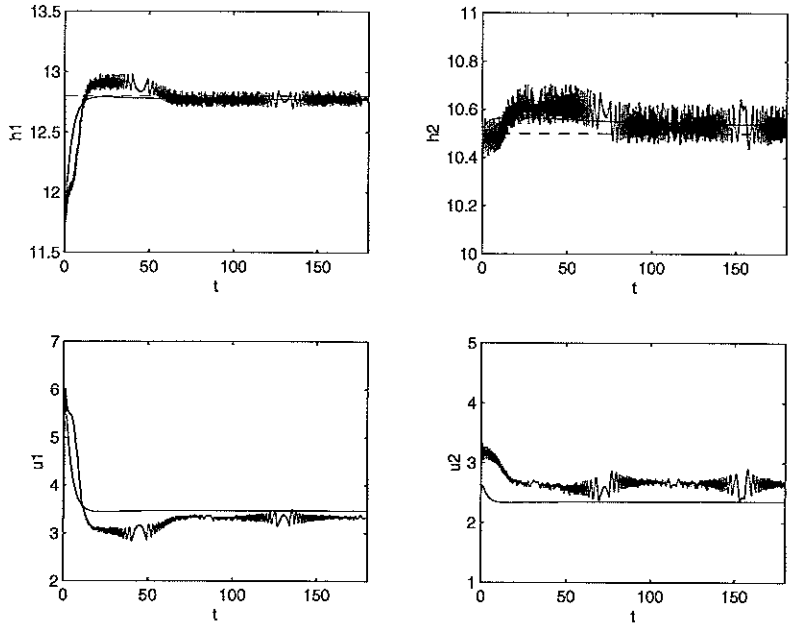

Figure 23 Minimum Phase LQG 3 Step Response: nonlinear model and the experiment.

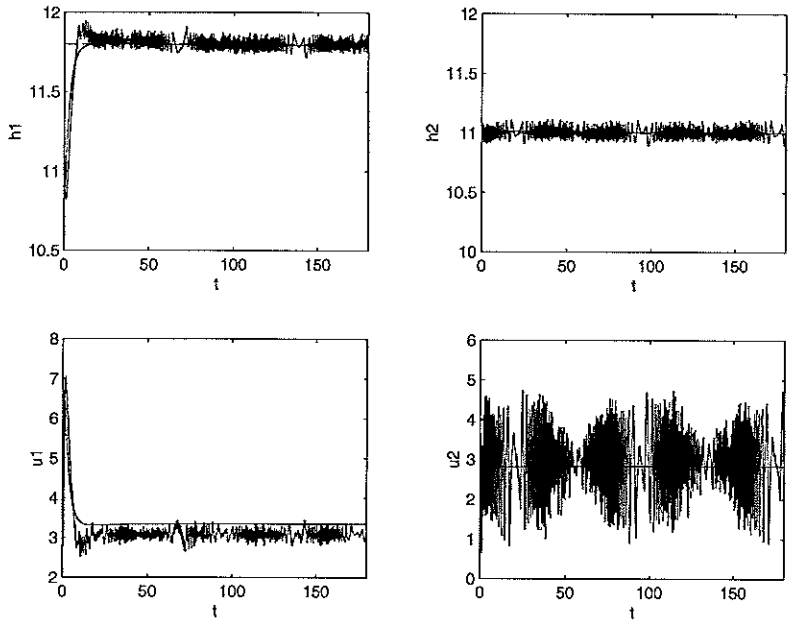

Figure 24 Minimum Phase H_∞ Step Response: nonlinear model and the experiment.

5.2 Disturbance Rejection

Minimum Phase Feedback linearization is found to have the best disturbance rejection properties in all measured characteristics, and MPC with $\beta = .5$ comes in a close second. Surprisingly, H_∞ produced some of the worst error norm characteristics which could indicate a poor choice in the selection

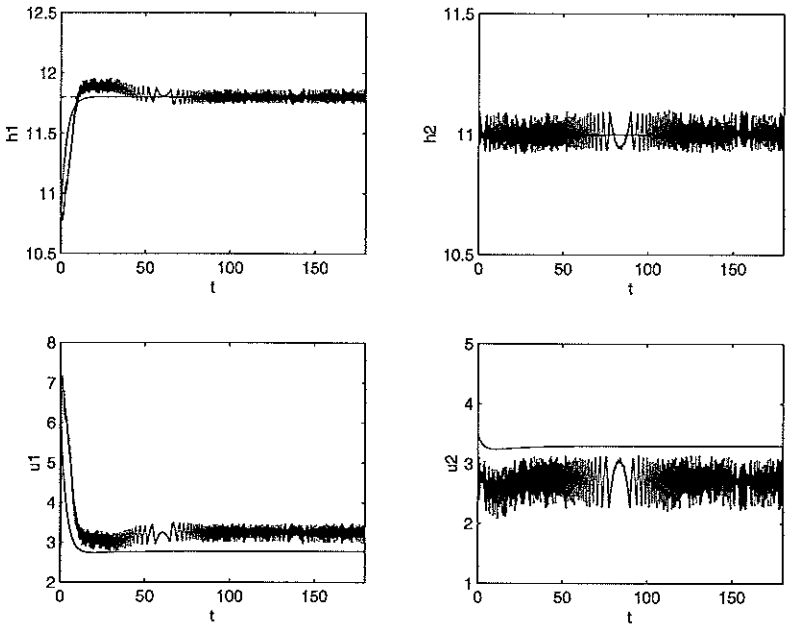

Figure 25 Minimum Phase Loop-Shaping Step Response: nonlinear model and the experiment.

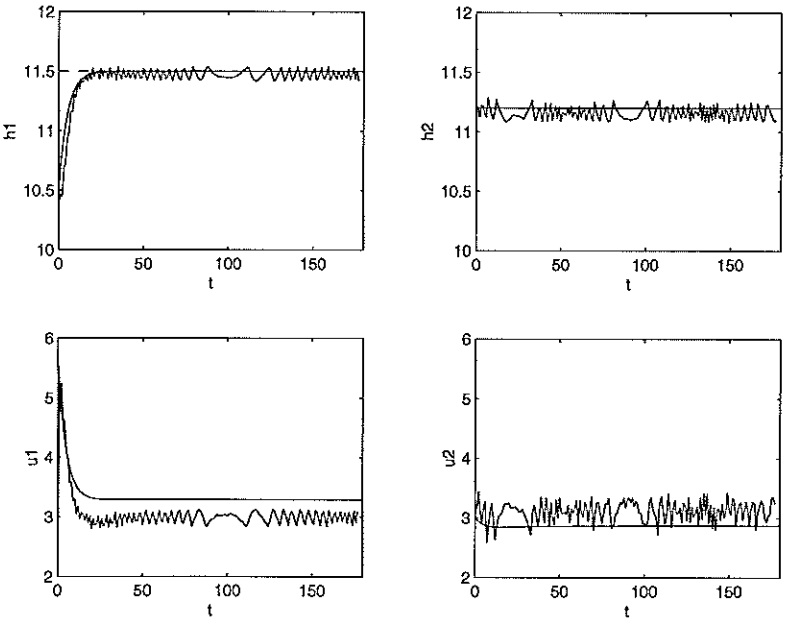

Figure 26 Minimum Phase Feedback Linearization Step Response: nonlinear model and the experiment.

of the weighting transfer functions.

Nonminimum Phase Table 7 shows the disturbance rejection properties of the nonminimum phase controllers.

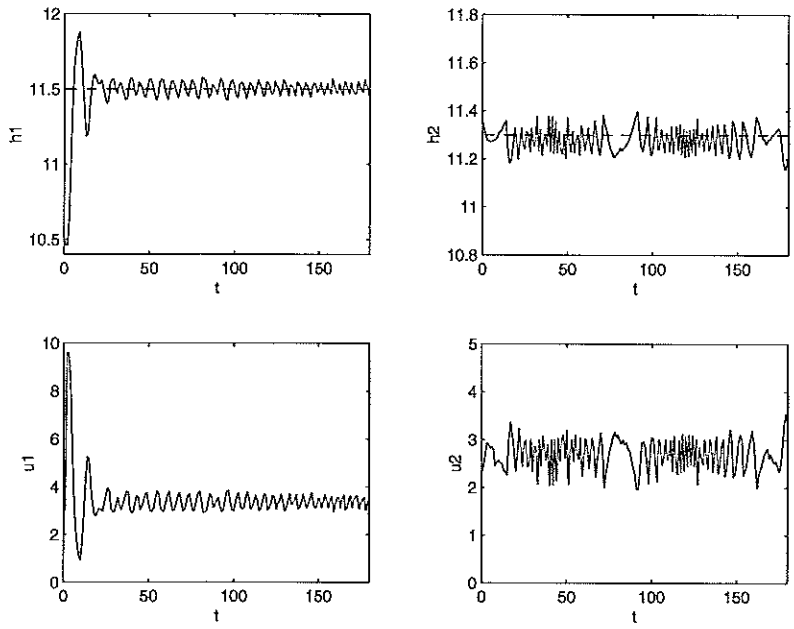

Figure 27 Minimum Phase MPC ($\beta = .5$) Step Response: the experiment.

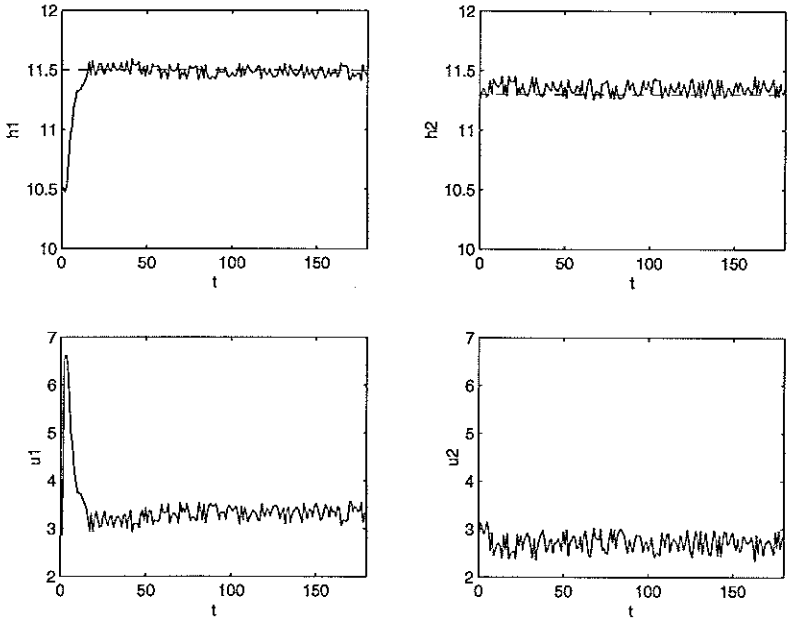

Figure 28 Minimum Phase MPC ($\beta = 2$) Step Response: the experiment.

	LQG 1	LQG 3	H_∞
t_r	200	170	160
M_p	30	7	25
t_s	850	800	500
ss e_1	15	0	0
$\|e_1\|_2$	11.73	8.91	14.16
$\|e_1\|_\infty$	1.14	1.04	1.49
$\|e_2\|_2$	7.10	9.65	11.44
$\|e_2\|_\infty$	0.62	1.06	1.20

Table 5 Experimental data for the step response in h_1 for the nonminimum phase plant.

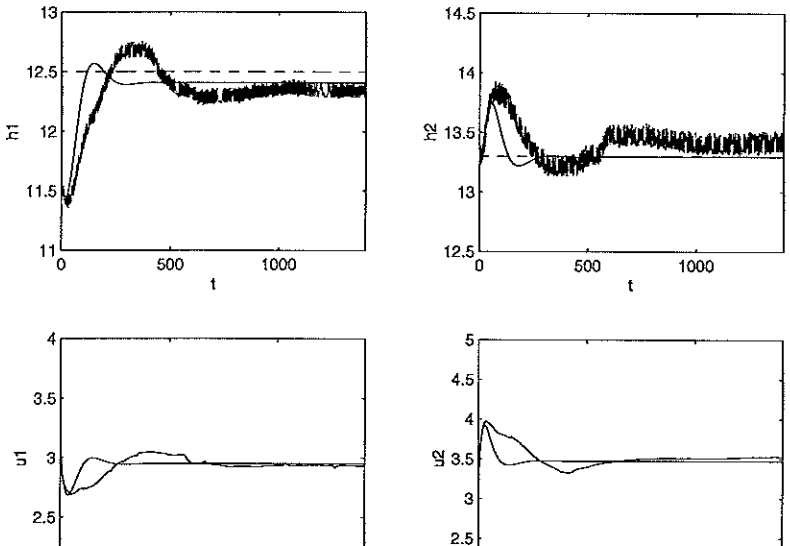

Figure 29 Nonminimum Phase LQG 1 Step Response: nonlinear model and the experiment.

	LQG 3	H_∞	lp-shp	fbk lin	MPC $\beta = .5$	MPC $\beta = 2$
$\|e_1\|_2$	1.83	5.99	4.53	.94	.98	1.55
$\|e_1\|_\infty$	.31	1.41	.97	.20	.22	.45
$\|e_2\|_2$	13.90	13.90	13.04	12.26	13.04	13.4
$\|e_2\|_\infty$	4.02	3.64	3.52	3.61	3.85	3.92

Table 6 Experimental data for the rejection of a disturbance in h_2 for the minimum phase plant.

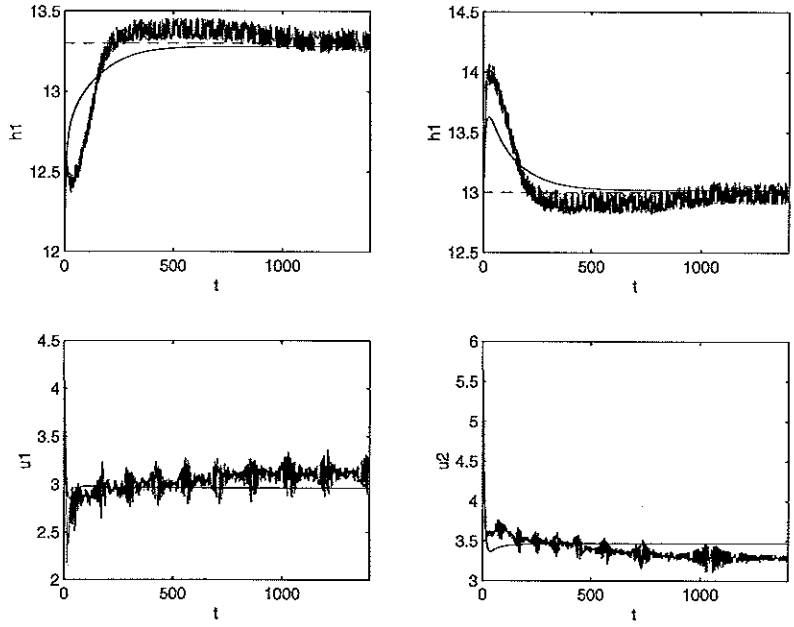

Figure 30 Nonminimum Phase LQG 3 Step Response: nonlinear model and the experiment.

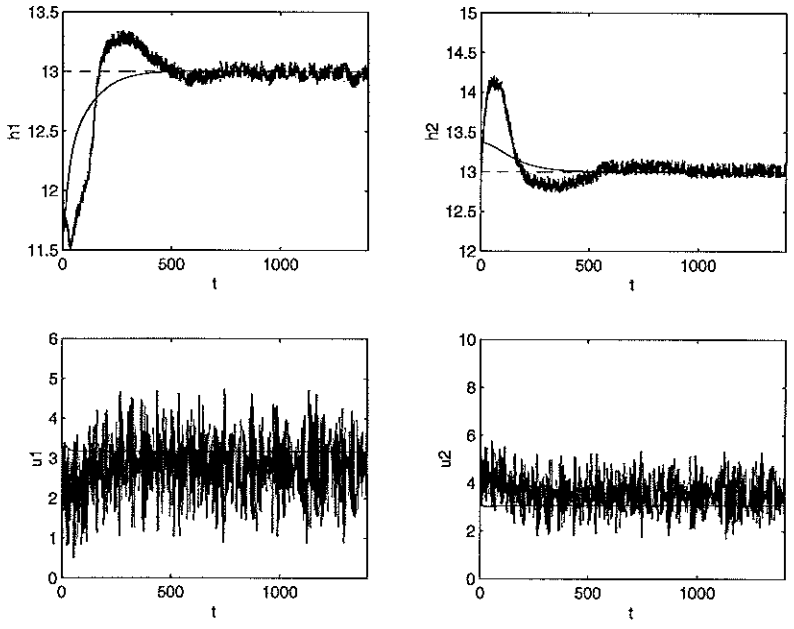

Figure 31 Nonminimum Phase H_∞ Step Response: nonlinear model and the experiment.

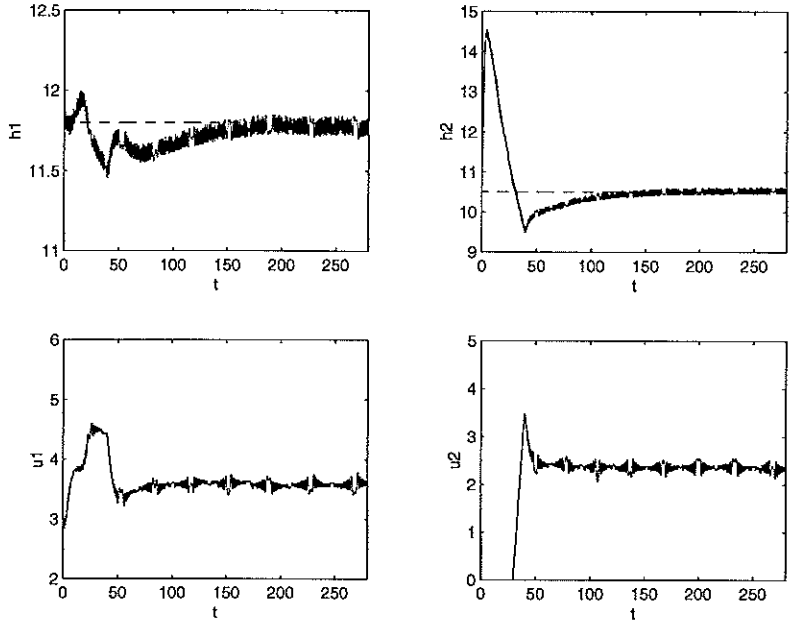

Figure 32 Minimum Phase LQG 3 Disturbance Rejection: the experiment.

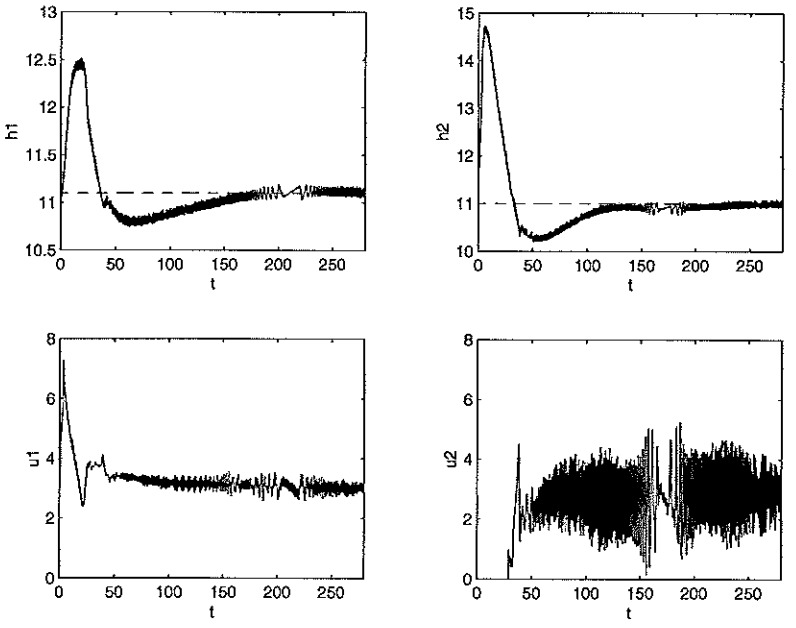

Figure 33 Minimum Phase H_∞ Disturbance Rejection: the experiment.

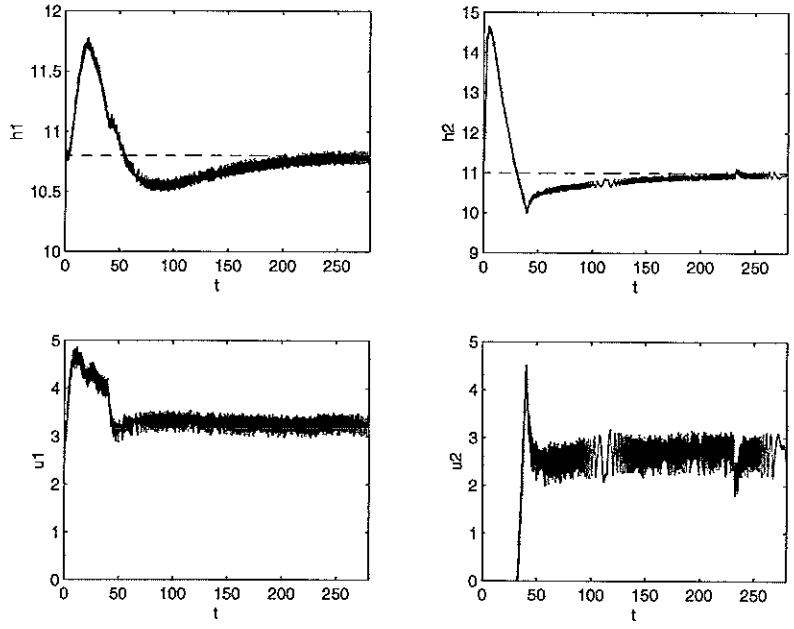

Figure 34 Minimum Phase Loop-Shaping Disturbance Rejection: the experiment.

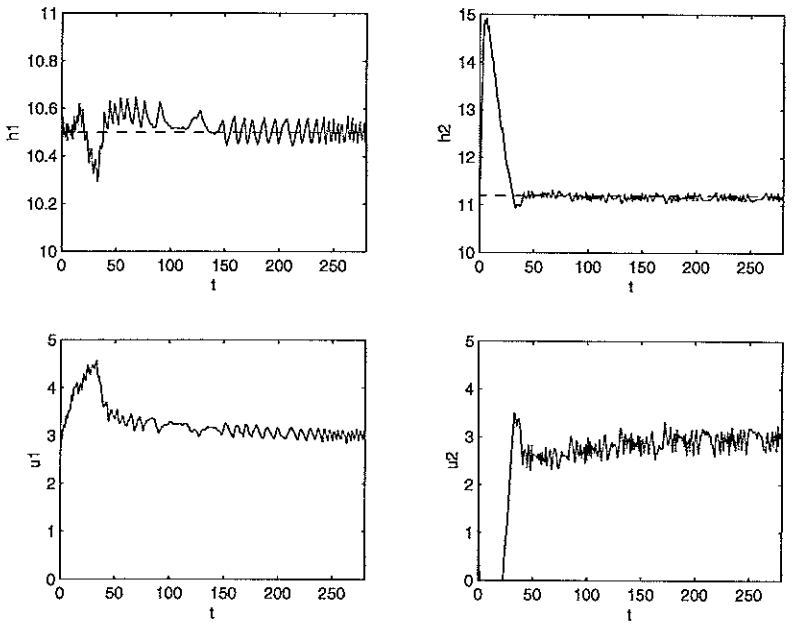

Figure 35 Minimum Phase Feedback Linearization Disturbance Rejection: experiment.

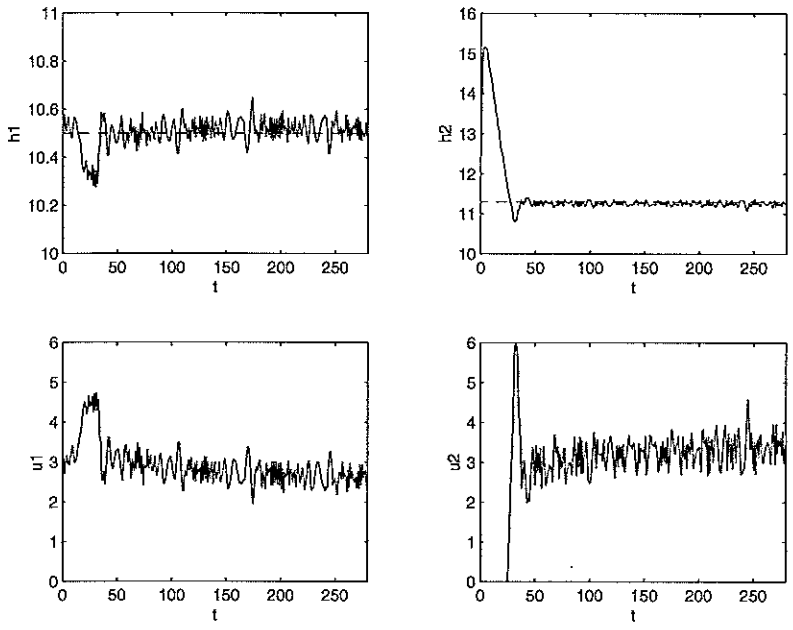

Figure 36 Minimum Phase MPC ($\beta = .5$) Disturbance Rejection: the experiment.

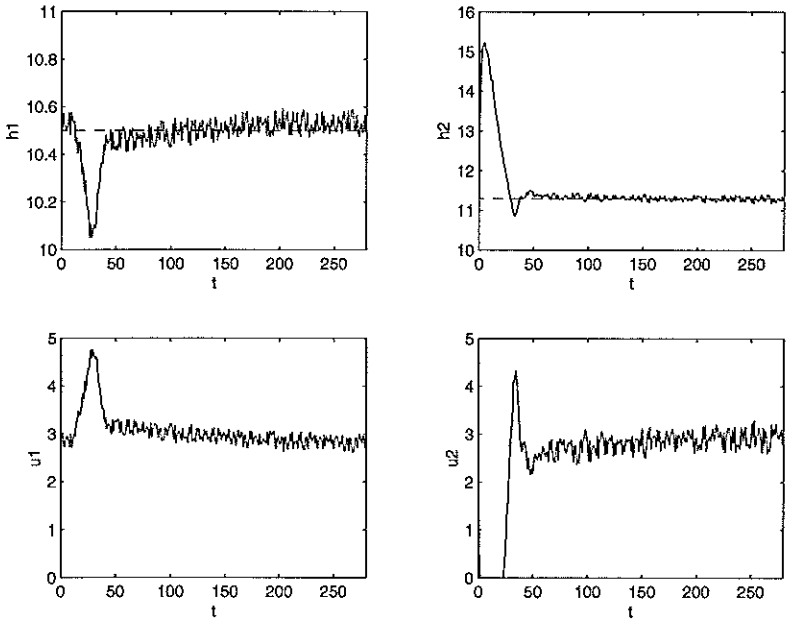

Figure 37 Minimum Phase MPC ($\beta = 2$) Disturbance Rejection: the experiment.

	LQG 3	H_∞
$\|e_1\|_2$	16.55	20.08
$\|e_1\|_\infty$	2.06	2.48
$\|e_2\|_2$	19.57	28.61
$\|e_2\|_\infty$	3.85	4.94

Table 7 Experimental data for the rejection of a disturbance in h_2 for the nonminimum phase plant.

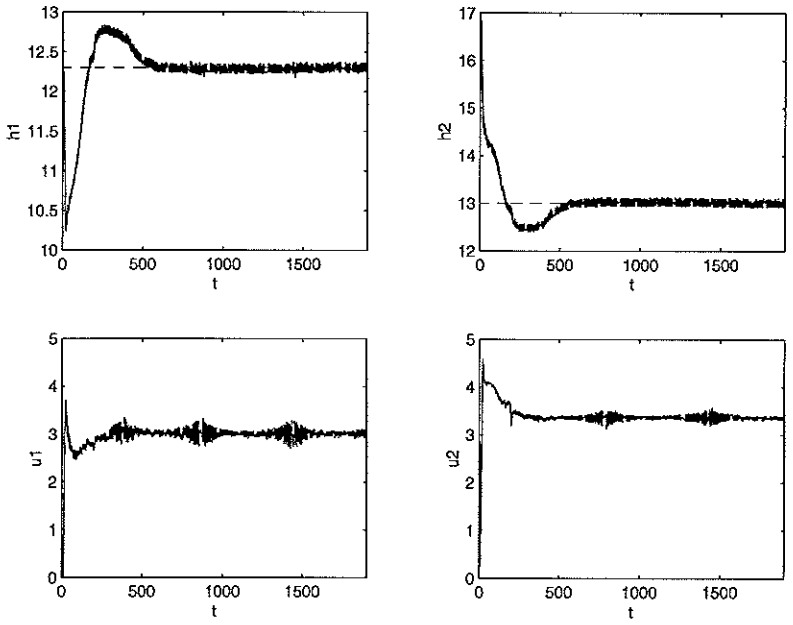

Figure 38 Nonminimum Phase LQG 3 Disturbance Rejection: the experiment.

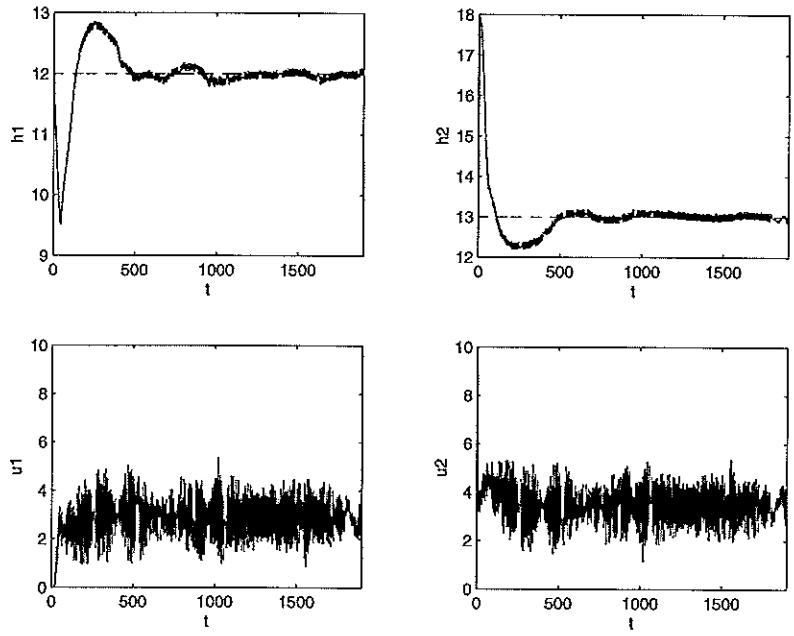

Figure 39 Nonminimum Phase H_∞ Disturbance Rejection: the experiment.

6. Summary

- Almost all minimum phase controllers produced step responses which were decently better than the decentralized PI controller already documented. As expected with the nonminimum phase plant, not all methods worked, but those which did work produced responses which were significantly better than those of decentralized control.
- The effects of the RHP zeros appeared in many different ways.
  - For all stable controllers, the RHP zero resulted in a reduction in bandwidth.
  - On the simpler control methods attempted, the RHP zero resulted in unstable dynamics.
  - The RHP zero indirectly caused MPC methods to fail by creating a need for extended computation time due to the low bandwidth.
- The experimental evidence does not give much evidence that the performance limitations of RHP MIMO zeros can be distributed among the different loops and thereby reduced. One of the only small pieces of evidence is that the RHP zero was slightly within the bandwidth for some controllers. This fact does not prove much because there is no data on how a SISO system would respond with the same RHP zero location and bandwidth.
- The notable difference between the working nonminimum phase controllers discussed in this paper and the decentralized PI controller is the anti-diagonal characteristic of these new controllers' transfer matrix. This characteristic can easily be seen in the step responses: A step in the height of tank 1 (h_1) results in a large control input from pump two (u_2). This characteristic comes from the fact the nonminimum phase plant has a highly anti-diagonal transfer matrix.
- All the minimum phase controllers produced comparable results, despite the varying degrees of complexity. For the linear controllers, loop-shaping produced good responses with four states, LQG with six states, and H_∞ with as many as 28 states. The linear responses were not much different from the nonlinear responses, although nonlinear methods did have a couple of better characteristics. The only minimum phase control which was noticeable slower than the rest is the decentralized controller.
- The results of MPC depend significantly on two factors: the computation time (or efficiency) and the relative weight of the inputs compared to the errors in the $E(u)$. When the algorithms are so inefficient that only one step into the future is predicted, even the minimum phase plant is unstable. The computation time needed for the nonminimum phase plant was great enough that no stable controllers were produced. The relative weights of the inputs compared to the errors shaped the response with respect to rise time, oscillations, and DC offset.
- The special case of depend stationary tank flow corresponding to the movable zero located at the origin was examined briefly with LQG and H_∞ methods. Although these methods seem to produce good controllers during the design process, responses were found to be unstable even in linear simulations.

- Integrators make a large difference in the LQG design method, especially for the nonminimum phase plant. Direct LQG design of the non-augmented plant produced clearly the worst responses of all the stable controller. Simply designing the LQG controller about a plant augmented integrators produced one of the best controllers for the nonminimum phase system.
- Feedback linearization was the only control scheme designed about the nonlinear dynamics. The MPC algorithms could have also been designed about the nonlinear dynamics, but only a linearized version was used in this paper.
- MPC produced some very good responses for the minimum phase, despite the fact it was based on a linear model: Its step response was very fast and its disturbance rejection was one of the best.